CHAPTER 3
SIMPLY-SUPPORTED CYLINDER ACOUSTIC RESPONSE

In this chapter the internal acoustic response of a simply-supported (SS) cylinder is addressed. The acoustic response is based on a boundary element formulation of the Kirchoff-Helmholtz integral (Fahy, 1985). The application of the K-H integral to compute the internal acoustic response of a cylinder is reviewed. In order to verify the boundary element model, an analytical solution to the acoustic response of a cylinder vibrating with a single mode structural vibration is derived. The results from the analytical solution and the boundary element model are then compared. In Chapter 4 the boundary element model is further verified experimentally using the simply-supported cylinder described in Chapter 2. Once the acoustic model is validated, it can be used to predict the internal acoustic response of a large scale cylinder which emulates a rocket payload fairing (PF).

3.1 Kirchoff-Helmholtz Integral Applied to a Cylinder

A great deal of work has been performed on the acoustic radiation problem. However, the solution of the internal problem has not received as much attention (Cheng, 1994, Vlahopoulos, 1994, Kipp and Bernhard, 1987, Sybert and Cheng, 1986, Fahy, 1985, Francis and Sadek, 1985). In this section the analytical solution of the internal acoustic response of a vibrating cylinder is considered based on the Kirchoff-Helmholtz (K-H) integral.

If the structural surface vibration is the only source of acoustic energy, the K-H integral is given by (Fahy, 1985):

$$p(\vec{r}) = c(\vec{r})\int_S \left(p(\vec{r}_s)\frac{\partial G(\vec{r}_s,\vec{r})}{\partial n} + \imath\omega\rho\dot{w}_n(\vec{r}_s)G(\vec{r}_s,\vec{r}) \right) dS \tag{3.1}$$

$$c(\vec{r}) = \begin{cases} 1 & \textit{within the Volume} \\ 2 & \textit{on the boundary of the Volume} \end{cases} \tag{3.2}$$

where, $p, \vec{r}, \vec{r}_s, n, \rho, \dot{w}_n, \imath, \omega, S, \& \ G$, represent the pressure, field point location, surface point location, outward normal to the local field surface, density of the fluid medium (air), local normal surface velocity, imaginary number, angular frequency, surface area, and acoustic Green's function, respectively. The Green's function must satisfy the acoustic wave equation and the far-field radiation conditions. The K-H integral can then be directly integrated to solve for the acoustic field generated by a structure as long as the surface velocity and the surface pressure is known. Generally the spatial surface velocity of a structure can be measured or determined via finite element analysis or using analytical techniques. However, the spatial surface pressure is not easy to measure and is difficult to calculate. For the external radiation problem, the Green's function that is chosen is the free-field Green's function. For the internal acoustic problem, a convenient form of the Green's function can facilitate in solving for the internal pressure field within a closed space. By choosing the Green's function such that,

$$\frac{\partial G(\vec{r}_s,\vec{r})}{\partial n} = 0 \tag{3.3}$$

the first term of the integral in Eq. 3.1 is eliminated and the calculation of the surface pressure is no longer required. Therefore the pressure field can be solved by simply knowing the normal surface velocity of the structure. The Green's function that satisfies Eq. 3.3 is expressed in terms of the acoustical modes of the cavity and is given by:

$$G(\vec{r}_s,\vec{r}) = \sum_{ijk}^{\infty} \frac{\psi_{ijk}(\vec{r})\psi_{ijk}(\vec{r}_s)}{\Lambda_{ijk}(\kappa_{ijk}^2 - \kappa^2)} \tag{3.4}$$

where ψ, κ, Λ and subscript ijk are the internal acoustic mode shape, wavenumber, modal normalization constant, and modal indices, respectively (Fahy, 1985). For complicated geometries, the acoustic mode shape is difficult to compute and so direct calculation of Eq. 3.1 is generally not possible. However, for a rigid, finite, closed cylinder the acoustic mode shapes and eigen values are known. For a cylindrical cavity the acoustic mode shapes can be expressed in terms of cosine functions in the axial direction and Bessel functions in the radial direction. The acoustic mode shape is given by:

$$\psi_{ijk} = J_j(\lambda_{jk}\, r/R_{ac})\cos(i\pi x/l_{ac})\cos(j\theta) \tag{3.5a}$$

where, J represents a j^{th} order Bessel function, λ, R_{ac}, l_{ac} are the associated roots of the Bessel function (Blevins, 1987, Abramowitz and Stegun, 1970) and the internal radius and length of the cylinder, respectively. The modal normalization constant is the mean square value of the acoustic mode shape multiplied by the volume of the cylinder. For a cylindrical duct the mean square value of the 2-D mode shape is given for its cross section (Morse and Ingard, 1968). This expression can be multiplied by the cylinder's axial mode shape and integrated over the length of the cylinder to yield:

$$\Lambda_{ijk} = \int_V \psi_{ijk}^2(\vec{r})dV = \frac{J_j^2(\pi q_{jk})}{\varepsilon_i \varepsilon_j}\left\{1 - \frac{j^2}{(\pi q_{jk})^2}\right\} \tag{3.5b}$$

where,

$$\varepsilon_i, \varepsilon_j = \begin{cases} 1 & i = 0,\ j = 0 \\ 2 & i > 0,\ j > 0 \end{cases}$$

where V, J, q are the interior volume, Bessel function, and constants related to the roots of the Bessel function.

The coordinate system for the cylinder is presented in Figure 2.1. Using the Green's function defined by Eq. 3.4, Eq. 3.1 simplifies to the following integral:

$$p(\vec{r}) = c(\vec{r})\int_S \iota\omega\rho\dot{w}_n(\vec{r}_s)G(\vec{r}_s,\vec{r})dS \tag{3.6}$$

If it is assumed that the excitation is temporally harmonic, then Eq. 3.6 can be written in terms of the acceleration of the surface of the cylinder.

$$p(\vec{r}) = c(\vec{r})\rho \int_S a_n(\vec{r}_s) G(\vec{r}_s, \vec{r}) dS \tag{3.7}$$

Combining Eq. 3.4 and Eq. 3.7 produces:

$$p(\vec{r}) = c(\vec{r})\rho \int_S a_n(\vec{r}_s) \sum_{ijk}^{\infty} \frac{\psi_{ijk}(\vec{r})\psi_{ijk}(\vec{r}_s)}{\Lambda_{ijk}(\kappa_{ijk}^2 - \kappa^2)} dS \tag{3.8}$$

The expression can be rearranged since the integral of the summation is equivalent to the summation of the integrals over the modal indices ijk

$$p(\vec{r}) = c(\vec{r})\rho \sum_{ijk}^{\infty} \int_S a_n(\vec{r}_s) G_{ijk} dS \tag{3.9}$$

The mode shape for a rigid closed cylinder are then substituted into the appropriate Green's function and are expressed as:

$$G_{ijk} = \frac{\psi_{ijk}(\vec{r})\psi_{ijk}(\vec{r}_s)}{\Lambda_{ijk}(\kappa_{ijk}^2 - \kappa^2)} = \frac{\left\{J_j\left(\lambda_{jk}\, r/R_{ac}\right)\cos\left(i\pi x/l_{ac}\right)\cos\left(j(\theta - t_o)\right)\right\}\left\{J_j\left(\lambda_{jk}\right)\cos\left(i\pi x_s/l_{ac}\right)\cos\left(j(\theta_s - t_o)\right)\right\}}{\Lambda_{ijk}(\kappa_{ijk}^2 - \kappa^2)} \tag{3.10}$$

where, $t_o, x, r, \theta,$ and subscript s represent the angle that orients the mode shapes for a given excitation, axial, radial, and angular position within the cylinder, and the axial and angular position on the cylinder surface, respectively.

For a specified cylinder geometry, disturbance orientation, modal index, and location of calculation, the variables: $i, j, k, l_{ac}, x, \theta, t_o, \kappa, r, R_{ac}$ are given and the following variables are constant: $\lambda_{jk}, \kappa_{ijk}, \Lambda_{ijk}$

$$G_{ijk} = \left[\frac{J_j\left(\lambda_{jk}\, r/R_{ac}\right)\cos\left(i\pi x/l_{ac}\right)\cos\left(j(\theta - t_o)\right)J_j\left(\lambda_{jk}\right)}{\Lambda_{ijk}(\kappa_{ijk}^2 - \kappa^2)}\right]\cos\left(i\pi x_s/l_{ac}\right)\cos\left(j(\theta_s - t_o)\right) \tag{3.11}$$

CONSTANTS VARIABLES

Substituting Eq. 3.11 into Eq. 3.9 produces an expression in which the constants may be removed from the integral for each modal index ijk.

$$p(\vec{r}) = c(\vec{r})\rho\sum_{ijk}^{\infty} \frac{J_j\left(\lambda_{jk}\, r/R_{ac}\right)\cos\left(i\pi x/l_{ac}\right)\cos\left(j(\theta - t_o)\right)J_j\left(\lambda_{jk}\right)}{\Lambda_{ijk}\left(\kappa_{ijk}^2 - \kappa^2\right)} \times \int_S a_n(\vec{r}_s)\cos\left(i\pi x_s/l_{ac}\right)\cos\left(j(\theta_s - t_o)\right)dS \qquad (3.12)$$

Equation 3.12 can ultimately be used to calculate the internal acoustic response within a cylinder if the spatial accelerance of the interior surface is known. The motion of the cylinder surface can be determined using analytical methods, as described in Chapter 2, or by using finite element analysis.

3.2 Internal Acoustic Response of a Cylinder Having a Single Mode Structural Vibration

As the speed of computers continually increases, more and more engineers are relying on numerical analysis to solve complex physical problems. Acoustical analysis is no exception. Finite element analysis (FEA) and more often, boundary element analysis (BEA) are being routinely used to solve for the acoustic response of a vibrating structure. However, the use of these software packages has the potential to produce solutions that may appear to be correct to the untrained eye, and in reality be totally wrong (Bathe, 1998). The need to verify numerical acoustic modeling with known analytical solutions becomes more and more important. This section derives an analytical solution to the internal acoustic response of a simply-supported (SS) cylinder with rigid end-caps based on a single mode structural response. A comparison of the derived analytical solution with a numerical solution obtained by using boundary element analysis is presented in section 3.4.

The solution to the internal acoustic response of the cylinder (Eq. 3.12) requires knowledge of the spatial acceleration distribution of the interior surface of the cylinder. It should be reiterated that the true response or operating shape of the cylinder will be comprised of many individual modes and that a single mode will dominate only near its modal natural frequency. An assumption is now made about the spatial operating shape of the cylinder. If the structural response for a SS cylinder is approximated by a single mode vibration at a particular frequency, the spatial accelerance of the cylinder can be written as:

$$a_n(\vec{r}_s) = (a + \imath b)\sin(a_m \pi x_s / l_{ac})\cos\left(c_m(\theta_s - t_o)\right) \qquad (3.13)$$

where, c_m and a_m are the axial and structural modal indices and a and b are constants related to the magnitude and phase of the structural vibration. Combining Eq. 3.12 and 3.13 produces:

$$p(\vec{r}) = c(\vec{r})\rho\sum_{ijk}^{\infty} \frac{J_j\left(\lambda_{jk}\, r/R_{ac}\right)\cos\left(i\pi x/l_{ac}\right)\cos\left(j(\theta - t_o)\right)J_j\left(\lambda_{jk}\right)(a + \imath b)}{\Lambda_{ijk}\left(\kappa_{ijk}^2 - \kappa^2\right)} \times \int_S \sin(a_m \pi x_s / l_{ac})\cos\left(i\pi x_s/l_{ac}\right)\cos\left(c_m(\theta_s - t_o)\right)\cos\left(j(\theta_s - t_o)\right)dS \qquad (3.14)$$

Letting $dS = dx_s R_{ac} d\theta_s$, the surface integral (in Eq. 3.14) over the interior of the cylinder becomes:

$$R_{ac} \int_{\theta=0}^{\theta=2\pi} \int_{x=0}^{x=l} \sin(a_m \pi x_s / l_{ac}) \cos(i\pi x_s / l_{ac}) \cos(c_m(\theta_s - t_o)) \cos(j(\theta_s - t_o)) dx_s R_{ac} d\theta_s \qquad (3.15)$$

Evaluating the first integral produces the following expression:

$$\frac{R_{ac} l_{ac}}{2\pi} \left[\frac{1-\cos((a_m+i)\pi)}{a_m+i} + \frac{1-\cos((a_m-i)\pi)}{a_m-i} \right] \int_{\theta=0}^{\theta=2\pi} \cos(c_m(\theta_s - t_o)) \cos(j(\theta_s - t_o)) d\theta_s \qquad (3.16)$$

Subsequent evaluation of the second integral produces the following expression:

$$\frac{R_{ac} l_{ac}}{4\pi} \left[\frac{1-\cos((a_m+i)\pi)}{a_m+i} + \frac{1-\cos((a_m-i)\pi)}{a_m-i} \right] \times$$
$$\left\{ \frac{\sin(2\pi(j-c_m) + (c_m-j)t_o) - \sin((c_m-j)t_o)}{j-c_m} + \frac{\sin((c_m+j)t_o) - \sin((c_m+j)t_o - 2\pi(j+c_m))}{j+c_m} \right\}$$

Substitution of the above expression into Eq. 3.14 for the surface integral produces a closed form solution for the internal acoustic response of a SS cylinder:

$$p(\vec{r}) = \frac{c(\vec{r}) \rho R_{ac} l_{ac} (a + \imath b)}{4\pi} \sum_{ijk}^{\infty} \frac{J_j(\lambda_{jk} r / R_{ac}) \cos(i\pi x / l_{ac}) \cos(j(\theta - t_o)) J_j(\lambda_{jk})}{\Lambda_{ijk} (\kappa_{ijk}^2 - \kappa^2)} \times$$
$$\left[\frac{1-\cos((a_m+i)\pi)}{a_m+i} + \frac{1-\cos((a_m-i)\pi)}{a_m-i} \right] \left\{ \frac{\sin((t_o - 2\pi)(c_m - j)) - \sin((c_m-j)t_o)}{j-c_m} + \right.$$
$$\left. \frac{\sin((c_m+j)t_o) - \sin((c_m+j)(t_o - 2\pi))}{j+c_m} \right\} \qquad (3.17)$$

if $a_m = i$, then $[\ ] = 0$

if $c_m = j$, then $\{\ \} = 2\pi + (1/j)\{\cos(j(2\pi - t_o)) \sin(j(2\pi - t_o)) - \cos(-jt_o) \sin(-jt_o)\}$

All the terms in the K-H integral (Eq. 3.1) have now been defined in terms of known quantities and the pressure within the cylinder can be determined directly. The result makes physical sense since the acoustic and structural modes for a cylinder can couple only if they have matching circumferential modal indices. Likewise, the axial modal indices have to be an even/odd combination for coupling to occur (Snyder and Hansen, 1994). For the acoustic response, direct integration of the K-H integral reduces the order of the problem as compared with using FEA. The analysis also circumvents calculating the surface pressure on the inside of the cylinder to determine internal acoustic response as is required by boundary element methods. Due to expanding the Green's function in terms of acoustic mode shapes, a singularity exists when the

excitation frequency coincides with an eigen frequency of the enclosed cavity. The singularity is a mathematical deficiency and does not exist physically, but can be handled by introducing a small imaginary component to the acoustic wave speed known as an acoustic loss factor (Silcox and Lester, 1989, Bullmore et al., 1987, Bullmore et al., 1986). The acoustic loss factor has not been well quantified and is the focus of Chapter 4.

3.3 Internal Acoustic Response of a Cylinder Using Boundary Element Analysis

Acoustic boundary element analysis (BEA) is based on the Kirchoff-Helmholtz (K-H) integral equation. The radiating structural surface is divided into a set of small discrete surface elements over which the pressure and normal surface velocity are considered constant. The surface integral is then evaluated using the elements on the boundary of the radiating structure. For the acoustic response, the use of the K-H integral reduces the order of the problem as compared with using acoustic finite element analysis. Also, since the mode shapes and Green's function for a closed, finite cylinder are known, the K-H integral for this problem can be directly integrated. If the geometry and mode shapes were obscure, the internal surface pressure would need to be calculated leading to additional complications (Vlahopoulos, 1992, Langley, 1991, Fyfe and Ismail, 1989, Kipp and Bernhard, 1987). This section will describe how the cylinder is partitioned to numerically evaluate the pressure within the cylinder for a given structural response.

To calculate the pressure within the cylinder at a specific point location, Eq. 3.7 is used. To compute a solution to Eq. 3.7 requires the integration of the product of the spatial structural accelerance and the Green's function. This integration is performed numerically by dividing the cylinder into discrete surface elements. Over each elemental area, the acceleration and local Green's function is assumed to be constant. The product of the local acceleration and Green's function is performed for each individual element and then summed for all of the elements. The summation is equivalent to the evaluation of the integral in Eq. 3.7. The acceleration response of the cylinder is determined at discrete points on its surface analytically, as described in Chapter 2 or measured directly, as described in Chapter 4. An example of the how the cylinder surface can be partitioned is shown in Fig. 3.1. The nodes in the figure indicate the location where the accelerance can be calculated or measured. For this case, the accelerance is known at eight positions axially and sixteen positions circumferentially (128 points total). Based on the known accelerance points, the cylinder surface area is divided into a set of discrete elements (128 elements) over which the normal surface accelerance and Green's function is considered constant. The discretization of the cylinder surface for this example is shown for the unwrapped cylinder in Fig. 3.2. For the acoustic results produced in Chapter 4, 12 axial elements and 36 circumferential elements are used to calculate the internal acoustic response of the cylinder based on the measured and calculated structural accelerance.

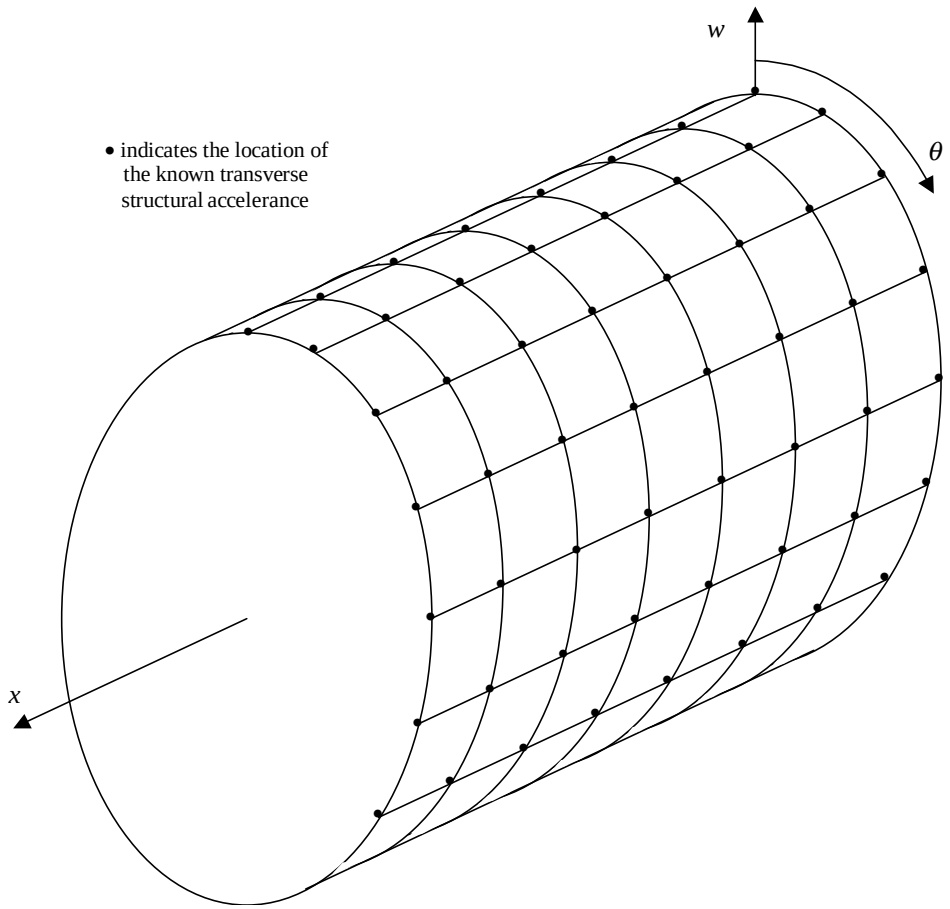

Figure 3.1 Example of the location of nodal accelerance points on the cylinder surface.

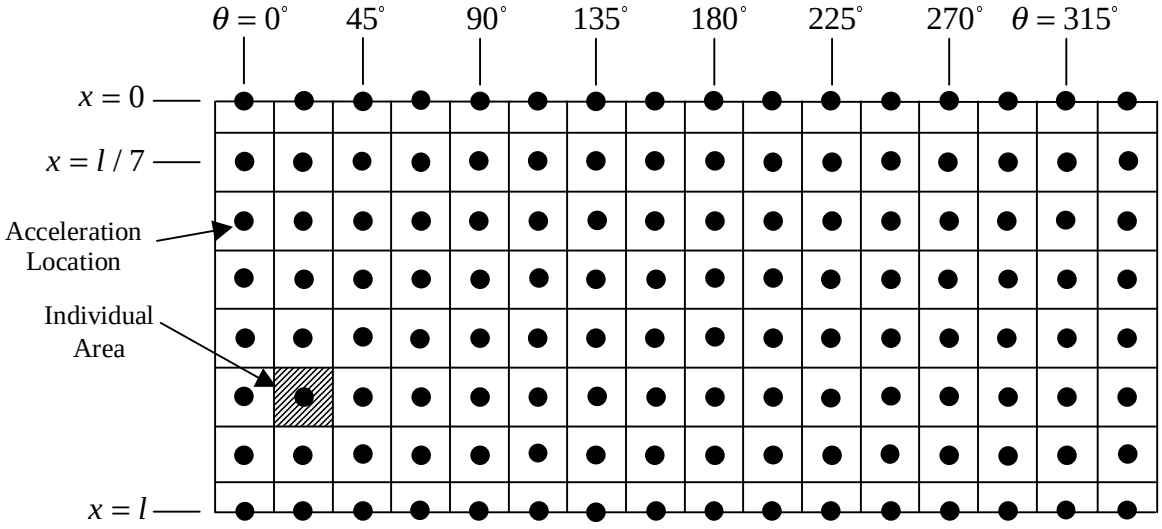

Figure 3.2 Corresponding example of the partitioned surface elements.

3.4 Analytical and Boundary Element Model Comparison for the Internal Acoustic Response of a Cylinder

In order to verify the analytical solution derived for the internal pressure of a cylinder, the result in Eq. 3.17 is compared to results obtained by performing a boundary element analysis (BEA), as described in section 3.3. The results from both solutions should ideally be identical. Two different comparisons are made and the properties of each case (case 1 and 2) are shown in Table 3.1.

The magnitude of the accelerance of the cylinder for case 1 is shown in Fig. 3.3. Since the cylinder is circular in shape, the response has been unwrapped so the accelerance can be plotted in Cartesian coordinates. The accelerance magnitude has also been phase-adjusted so its appearance is similar to what the physical displacement of the cylinder would actually be. The accelerance response shown in Fig. 3.3 corresponds to the operating shape that is near the (2,1) mode of the cylinder and can be expressed by Eq. 3.13.

Shown in Fig. 3.4 is the analytical internal acoustic response of the cylinder (vibrating with the properties described for case 1) for a radial slice at $x = 0.3l$. The minimum value of sound pressure level (SPL) is set to 40dB since the logarithm of zero is not defined. As is expected the acoustic response has four lobes about the circumference where the pressure is high. This makes physical sense since there has to be continuity between the internal pressure and the cylinder surface velocity. The analytical internal acoustic response of the cylinder for a horizontal slice passing through the cylinder's center is not shown for case 1 since the pressure is zero there. Instead the analysis is repeated for case 1 except $t_o = 0^\circ$ instead of 45°. Thus the pressure antinode should appear at the horizontal and vertical axis of the cylinder. This result is presented in Figure 3.5 for a horizontal slice passing through the center of the cylinder.

The magnitude of the accelerance of the cylinder for case 2 is shown in Fig. 3.6. The accelerance response corresponds to the operating shape that is near the (3,2) mode of the cylinder. Shown in Fig. 3.7 is the analytical internal acoustic response of the cylinder (predicted by Eq. 3.17) for a radial slice at $x = 0.3l$. As is expected the acoustic response has six lobes about the circumference where the pressure is high. The analytical internal acoustic response of the cylinder for a vertical slice passing through the cylinder's center is shown in Fig. 3.8. Likewise, as expected the acoustic response has two lobes in the axial direction, which makes physical sense.

The internal pressure for case 1 and 2 was also solved using BEA. The boundary of the cylinder was divided into 10 elements along the length and 36 elements along the circumference (360 elements total). The maximum difference between the analytical and BEA solution is approximately 0.08 dB for case 1 and 0.6 dB for case 2. No figures are presented for the BEA because the results are virtually identical to the analytical solution. The analytical and BEA solution of the acoustic response was also shown to be equivalent as a function of frequency for a given structural excitation. This shows that the numerical solution and the analytical solution are in agreement. Presented in Chapter 4 is an experimental verification of the BEA model, using the SS cylinder described in Chapter 2.

Table 3.1 Case properties comparing analytical and BEA

Property	Case 1	Case 2
Frequency (Hz)	1400	2022
t_o (deg.)	45	0
l (m)	.4064	.4064
R_{ac} (m)	.1207	.1207
c (m/s)	343	343
a	50	25
b	-100	25
c_m	2	3
a_m	1	2
Max. Error (dB)	.084	.603

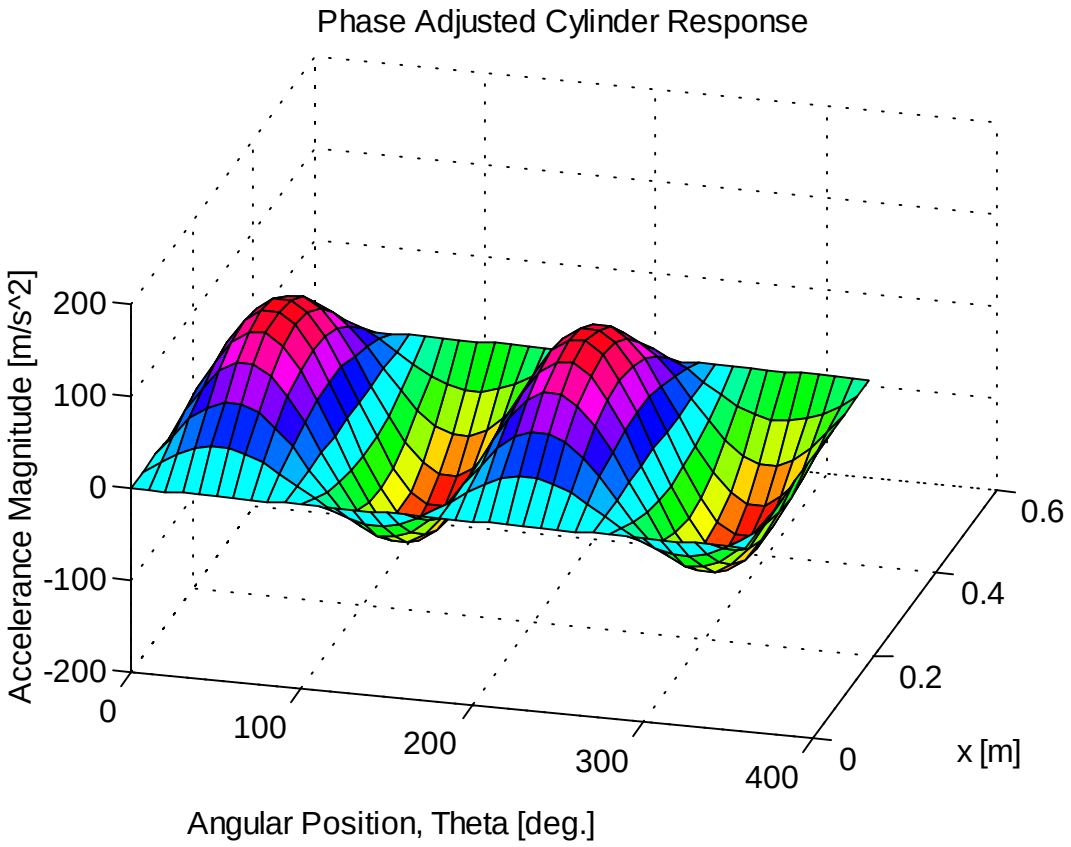

Figure 3.3 Magnitude of the cylinder accelerance (phase adjusted) for case 1.

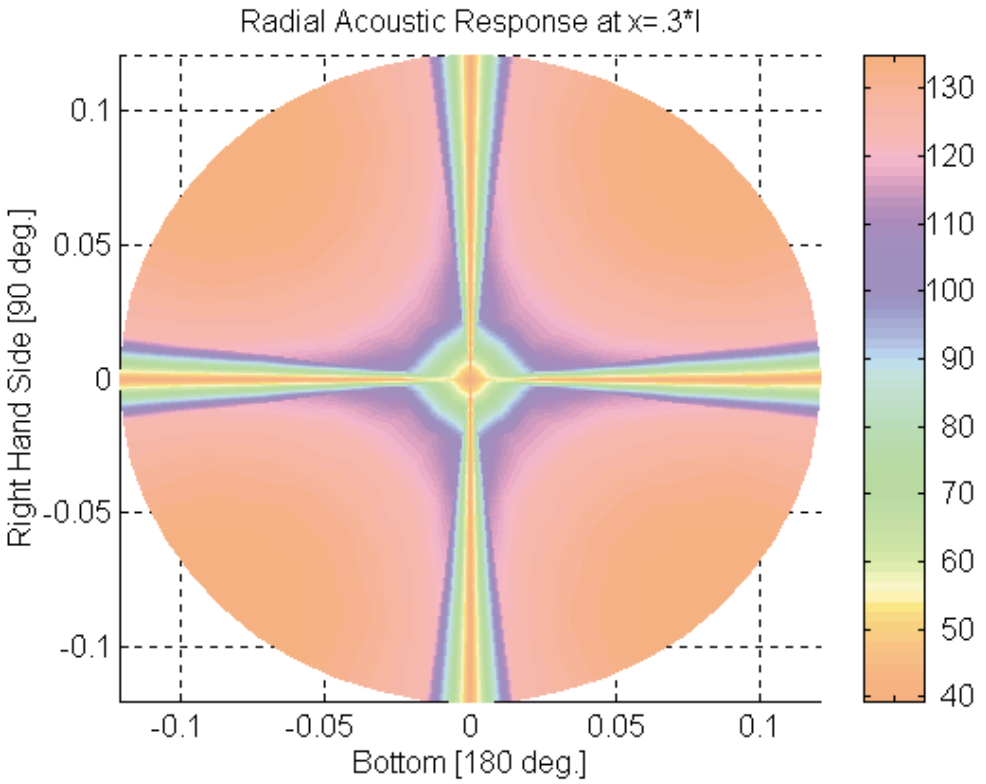

Figure 3.4 Radial acoustic response at $x = 0.3l$ for case 1 (SPL dB).

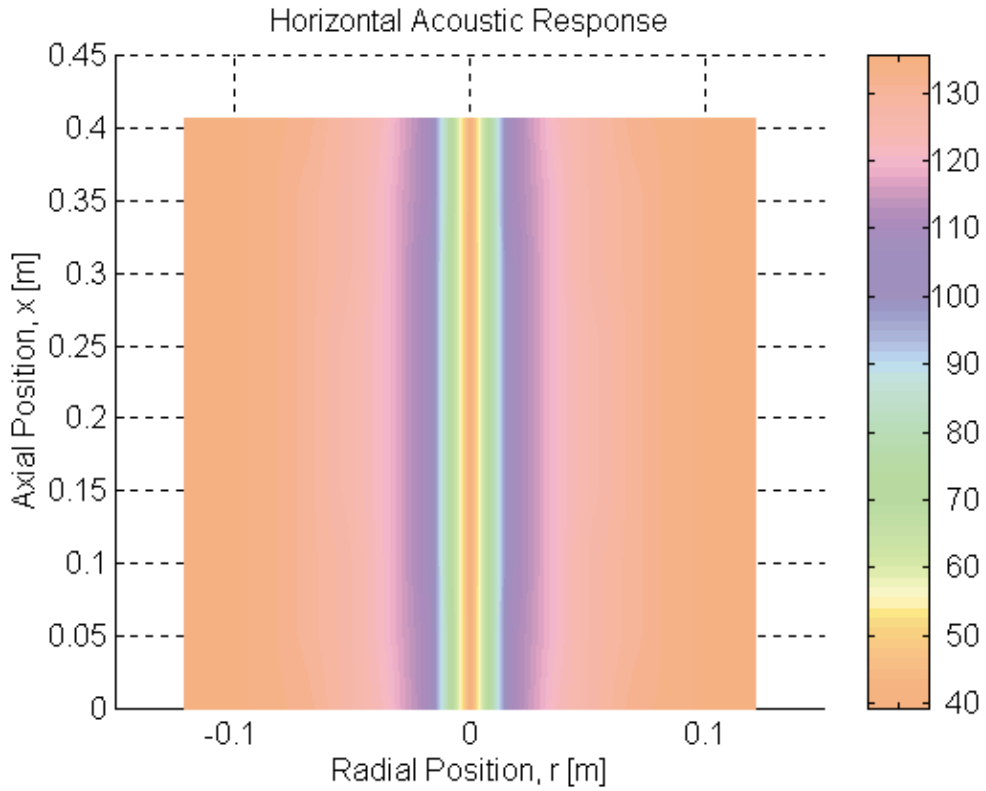

Figure 3.5 Horizontal acoustic response for case 1, except $t_o = 0^\circ$ (SPL dB).

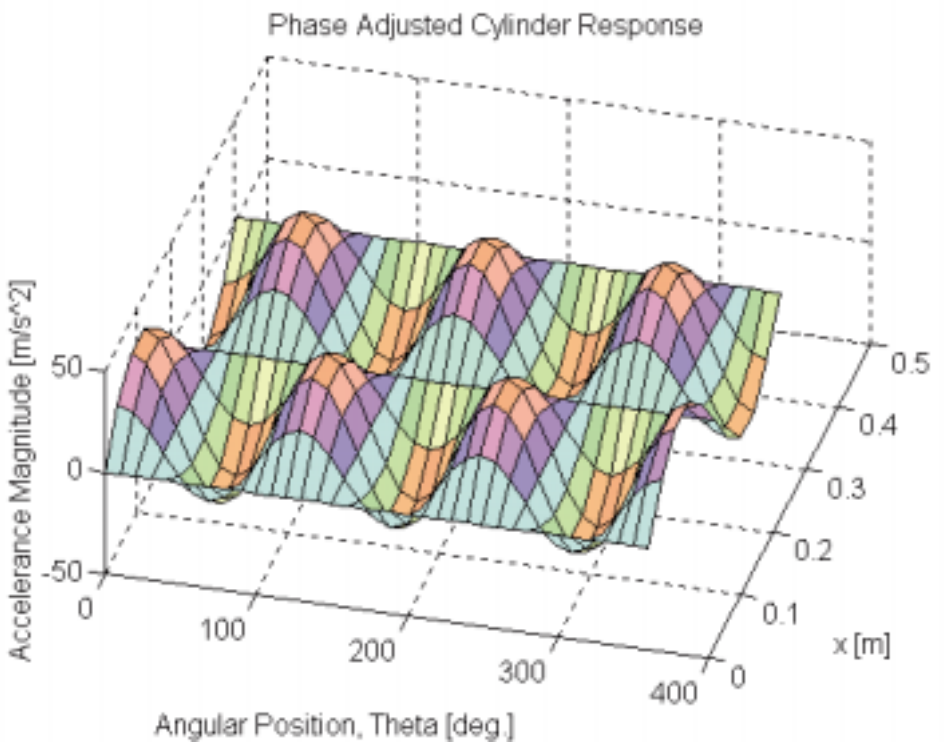

Figure 3.6 Magnitude of the cylinder accelerance (phase adjusted) for case 2.

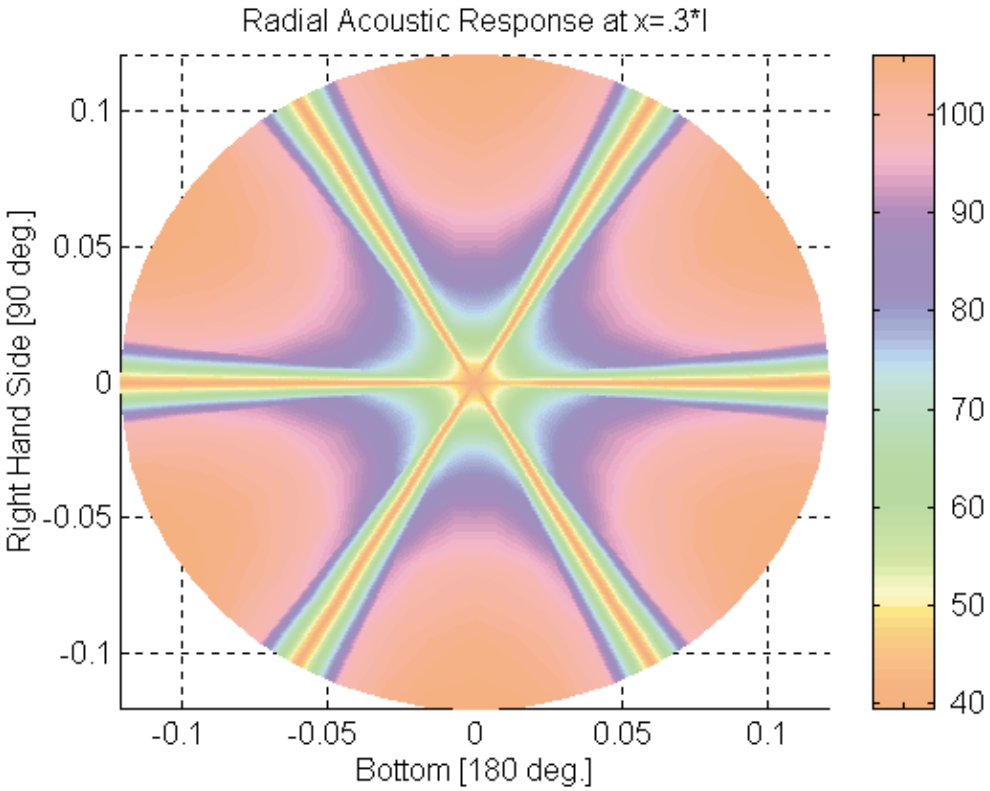

Figure 3.7 Radial acoustic response at $x = 0.3l$ for case 2 (SPL dB).

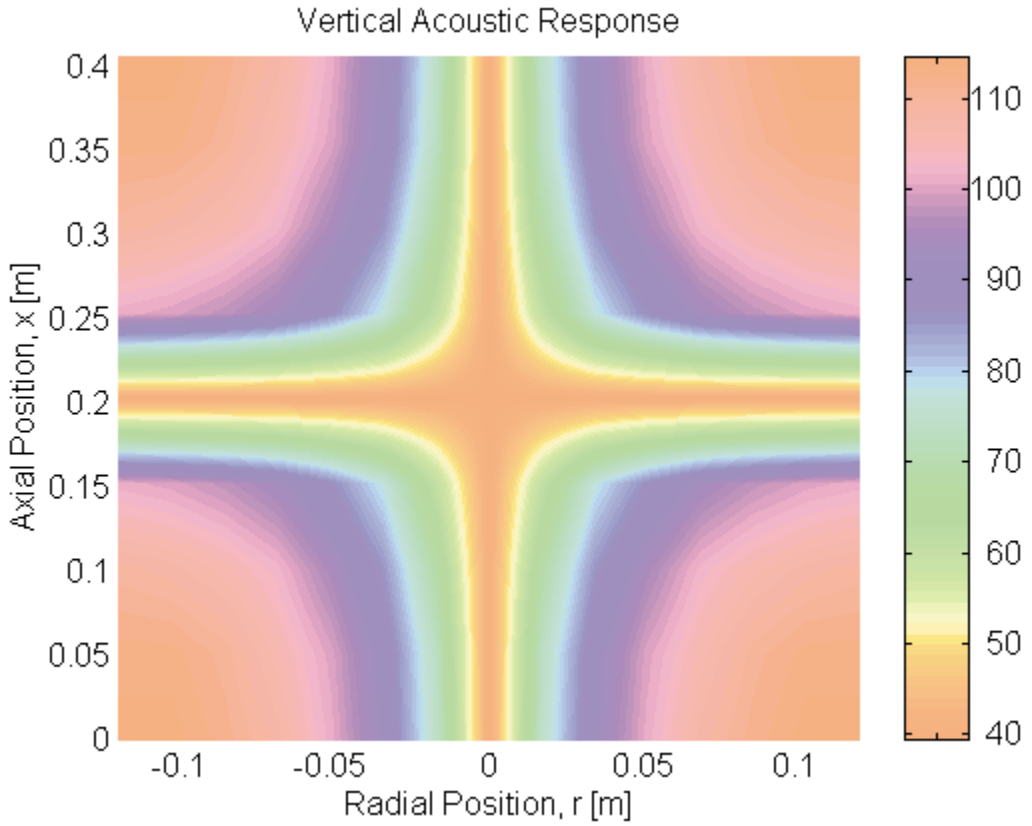

Figure 3.8 Vertical acoustic response for case 2 (SPL dB).

3.5 Variation of the Internal SPL with Applied Voltage

By perusing Eq. 3.17 it is possible to determine how the cylinder internal SPL changes, as the applied PZT actuator voltage is varied. From the result of the internal acoustic response of the cylinder, it is apparent that the internal pressure is proportional to the amplitude of the structural response, $(a+\imath b)$. It is also known that the amplitude of the cylinder structural response is proportional to the applied actuator loading. Since the force or moment generated by the PZT actuator varies linearly with the applied voltage, it can be concluded that the cylinder internal pressure is proportional to the applied PZT actuator voltage. This variation can be seen in Figs. 3.9 and 3.10 showing the variation of SPL with applied voltage. As the applied voltage increases linearly, the internal SPL varies logarithmically. If the applied voltage is doubled, the internal SPL will increase by 6 dB. Likewise if the applied voltage is increased ten times, the internal SPL will increase by 20 dB. This clearly is a limiting factor in using a PZT actuator to generate high internal SPLs.

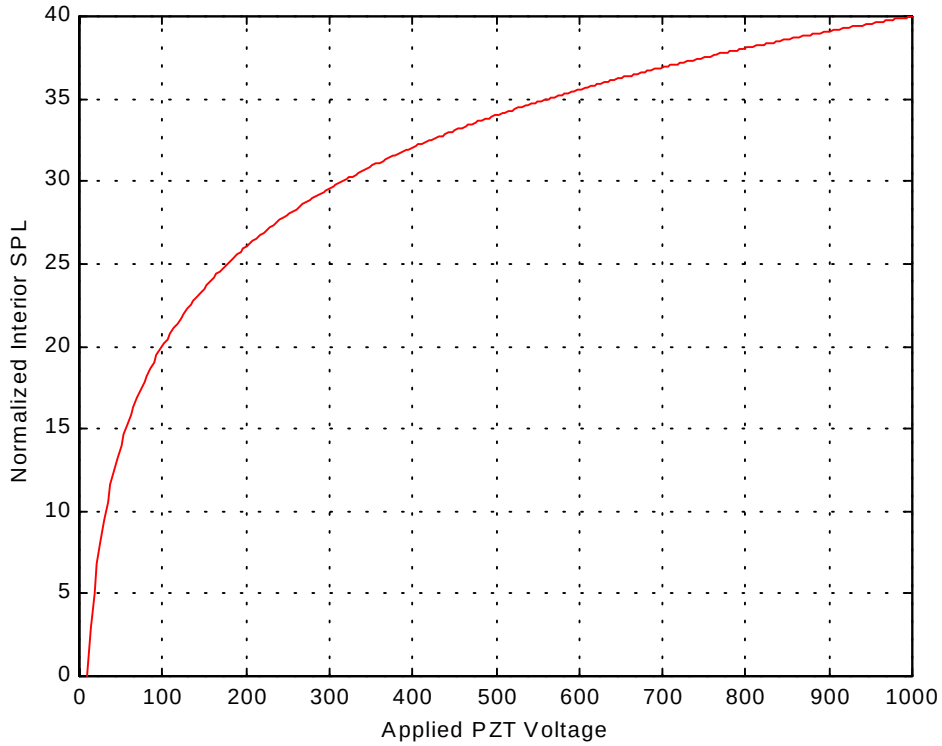

Figure 3.9 Normalized internal SPL for varying voltage, linear scale.

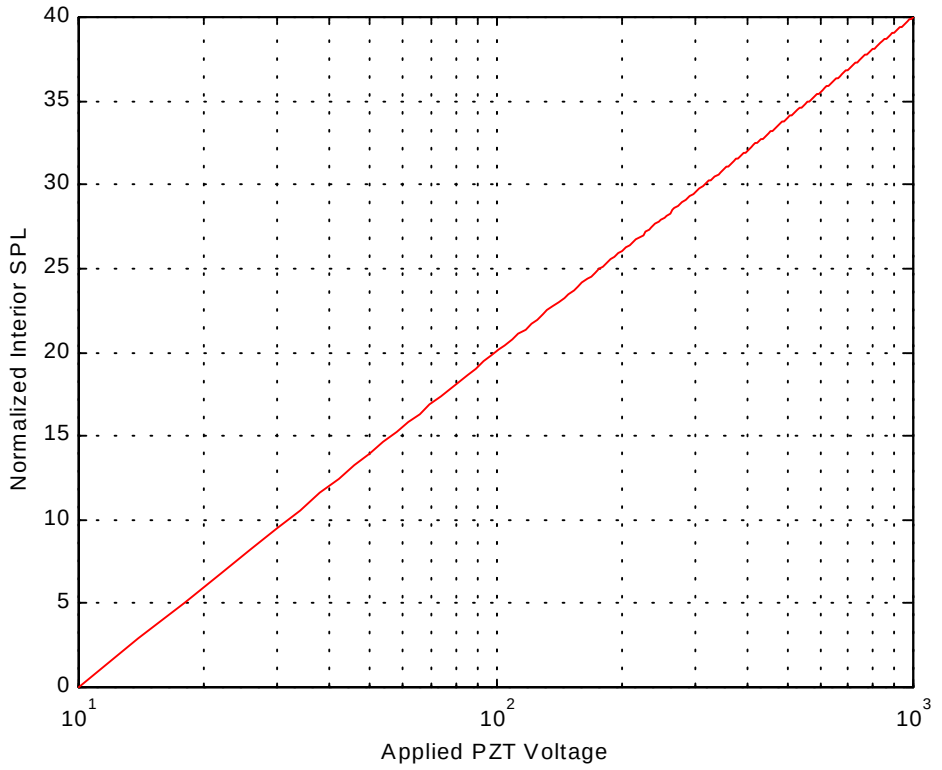

Figure 3.10 Normalized internal SPL for varying voltage, semi-log scale.